UNITED STATES DEPARTMENT OF THE INTERIOR
GEOLOGICAL SURVEY

Geological and Geochemical Data For Seamounts and Associated Ferromanganese Crusts in the Ratak Chain, Marshall Islands

by

W.C. Schwab[1], J.R. Hein[2], A.S. Davis[2], L.A. Morgenson[2]
C.L. Daniel[2], and J.A. Haggerty[3]

Open File Report 86-338

This report is preliminary and has not been reviewed for conformity with the U.S. Geological Survey editorial standards and stratigraphic nomenclature.

[1]Woods Hole, MA
[2]Menlo Park, CA
[3]University of Tulsa, OK

1986

INTRODUCTION

In 1984, the U.S. Geological Survey (USGS) conducted a reconnaissance cruise L9-84-CP aboard the R/V S.P. LEE along the northern Ratak Ridge, Marshall Islands (Fig. 1). Preliminary geochemical results from the cruise show that ferromanganese crusts (Mn crusts) on the submarine slopes of seamounts, and islands may have potential for commercial exploitation (Schwab and others, 1985). In this report we present shipboard data and laboratory analyses for rock samples collected on cruise L9-84-CP. This report should supplement the reports of Schwab and Bailey (1985) and Schwab and others (1985).

A total of 5410 km of 12-kHz and 3.5-kHz seismic-reflection data, and 730 km of 80-in^3 and 148-in^3 airgun seismic-reflection data were collected on cruise L9-84-CP (Schwab and Bailey, 1985). Eighteen sample stations were occupied; 13 dredge hauls and 3 box cores were collected (Table 1). These samples are available at the USGS Branch of Pacific Marine Geology offices in Menlo Park, California. Data presented in this report should encourage a more extensive field investigation and serious economic and technical evaluation of Mn crusts within the Marshall Islands area.

Ferromanganese-oxide precipitates that encrust hard substrate on the submarine flanks of seamounts, guyots, atolls, islands, and linear volcanic ridges, have been known for several decades (Cronan, 1977; Frazer and Fisk, 1980) but were not studied in a systematic way until the West German MIDPAC expedition of 1981 (Halbach and others, 1982). Unlike abyssal ferromanganese nodules, Mn crusts contain higher concentrations of the economically attractive metals, cobalt and platinum (Toth, 1980; Craig and others, 1982; Halbach and others, 1984; Hein and others, 1985). Mn crusts are predominantly hydrogenous in origin, in contrast to abyssal ferromanganese nodules which also have a substantial diagenetic input (Halbach and others, 1981).

In order for a Mn crust deposit to be economically attractive, it must be of high grade in recoverable metals, thick, and aerially extensive. During a 1984 workshop in Honolulu, East-West Center, engineers and geologists determined that Mn crusts must have an average thickness of 4 cm and a cobalt content greater than 0.8 percent of the dry weight (8000 ppm) to be considered for exploitation. The metals other than cobalt that are likely to be recovered from such a deposit include nickel, manganese, zinc, lead, phosphorous, and platinum. Preliminary chemical analyses of the Mn crusts collected during cruise L9-84-CP (Schwab and others, 1985) show that the average concentrations of metals within them are comparable with the mean metal contents of Mn crusts from the eastern Mid-Pacific Mountains and northern Line Islands Ridge, areas of high economic potential (Halbach and Manheim, 1984; Hein and others, 1985). Based on the extent of sea floor above 2400 m water depth and the age of the substrate, resource experts at the East-West Center in Honolulu placed the Marshall Islands as second in economic potential for Mn crusts as compared to the Mn crust resources within all other U.S. Pacific states, trust territories, and possessions (A.L. Clark, personal communication). Based on these and other geologic and oceanographic criteria, Hein and others (1986a) placed the Marshall Islands first with respect to U.S. interests.

For convenience, several previously unnamed seamounts have been named (see Hein and others, 1986b), including Erikub Seamount, Utirik Seamount, Bikar Guyot, and Ratak Guyot. We use these names informally in this report.

MAJURO ATOLL

Three dredge hauls were successfully conducted on the west flank of Majuro Atoll (Table 1 and Fig. 2). The average slope of this flank is approximately 8^{o}. Rocks recovered in dredge D2 are from a reef-front deposit with well-preserved shell and coral debris. Interpretation of seismic profile A (Figs. 3 and 4) suggests that the reef-front talus is approximately 20-m-thick and covers the acoustic basement in water depth of 1400 to 2100 m. Rocks recovered in dredge hauls D1 and D3 suggest that the acoustic basement depicted on profile A is a volcanic breccia with a phosphatized calcareous matrix (sample D1) and is overlain by a thin(?) blanket of volcanic and carbonate talus (sample D3).

The clasts found in the volcanic breccias that were collected in dredge haul D1 are predominately alkali olivine basalt fragments (see Tables 2 and 3 for substrate mineralogy and chemistry). Abundant glass found in these rocks indicate rapid quenching. Some wedge-shaped pieces of basalt contain palagonite rinds, suggesting autobrecciation, and contact rims of zeolites grading into the limestone matrix indicate the interaction of hot lava with wet sediment. The subrounded tachylitic basalt cobble recovered in dredge haul D3 suggests that subaerial eruption occurred, followed by erosion. Foraminifera found in the phosphatized carbonate matrix of samples recovered in D1 have been tentatively dated as Cretaceous.

Seismic-reflection profile A indicates that the western flank of Majuro Atoll is a site of mass wasting. The absence of Mn crust on rocks collected in D3 and the relatively thin crusts (average thickness <1 mm) on rocks collected in D1 and D2 may be a result of this mass wasting. It has been reported on other sea-floor edifices that Mn crusts tend to be thin where evidence of mass movement is especially strong (Hein and others, 1985). The dominant mineral in these and all Mn crusts sampled in the Marshall Islands is δMnO_2 (Table 5). Although the crusts are thin, the cobalt contents of the crusts from Majuro Atoll are quite high, averaging about 1 wt.% (Table 4).

ERIKUB SEAMOUNT

Two dredge hauls, D4 and D6, were successful on the south flank of Erikub seamount (Fig. 2). Seismic-reflection profile B indicate that both the north and south flanks of Erikub seamount have an average slope of 21^{o} (Figs. 3 and 5). Rocks collected in D6 (Table 1), approximately 15-km-east of seismic-reflection profile B (Figs. 3 and 5) in a water depth of 2900 m, suggest that the acoustic basement of profile B is composed of volcanic breccia and a phosphatized limestone matrix (Tables 2 and 3). A 130-m-thick talus deposit occurs at the base of the southern flank (Fig. 5). Rocks collected from this talus deposit (D4) include volcanic breccias with rounded clasts, in places surrounded with a thin Mn crust and intraclasts of biomicrite. Textures suggest that these breccias are debris-flow deposits. Some volcanic rocks collected on Erikub Seamount are zeolitized and may be replaced ash, suggesting a subaqueous flow origin. The abundance of highly vesicular tachylitic lapilli, oxidized hawaiites, and a variety of well-rounded clasts

indicate that the volcanic breccias collected in D4 and D6 resulted from subaerial eruption and erosion before deposition as submarine debris flows. Foraminifera from the phosphatized limestone matrix have been tentatively dated as Cretaceous.

The Mn crusts vary from thin coatings to crusts as thick as 6 mm on rocks collected in D4; while Mn crusts as thick as 4 cm, averaging 3 cm, coat rocks recovered from D6 (Table 1). Mn crusts that have smooth and polished surfaces indicate abrasion, probably by bottom currents or sediment gravity flows. Cobalt averaged about 0.51 wt.% in the Erikub Seamount Mn crusts (Table 4). Carbonate apatite occurs in one Mn crust and quartz is present in most (Table 5).

JEMO ISLAND

One successful dredge haul (D10), out of three attempts, yielded approximately 2 kg of rounded limestone cobbles from the south flank of Jemo Island (Fig. 2; Tables 1 to 3). Seismic-reflection profile C shows that the west and northeast flanks of Jemo Island have a hummocky surface on average declivities of 13° and 10°, respectively (Figs. 3 and 6). Slight acoustic penetration on the flanks and the presence of a talus deposit at the base of the west and northeast flanks suggest that the submarine flanks of the island are blanketed by carbonate mass-wasting deposits. Mn crusts from this edifice were not analyzed for chemical composition because they were too thin to isolate from the substrate.

UTIRIK SEAMOUNT

Three dredge hauls were recovered from Utirik Seamount, a steep-sided edifice that has slopes greater than 20° and a relatively flat summit that is blanketed by about 35 m of sediment (Figs. 3 and 7, Profile D). Dredge hauls D12, D13, and D14 (Fig. 2) yielded Mn crusts as thick as 30 mm but substrate was not recovered (Table 1). The average cobalt content in these crusts is high, about 0.85 wt.% (Table 4).

Although not sampled, the west flank of Utirik Seamount and the area between Utirik Seamount and Utirik Atoll appears to be covered with volcanic(?) pinnacles (Fig. 7).

BIKAR GUYOT

One successful dredge haul (D15) was recovered on the east flank of Bikar Guyot (Fig. 2). The east and west flanks of Bikar Guyot display a declivity of approximately 25° in water depth less than 2000 m, becoming gentler with increasing water depth (Figs. 3 and 8). Both 3.5-kHz and 148-in^3 airgun seismic-reflection profiles show no evidence of sediment or talus deposits on the flanks of Bikar Guyot.

Dredged rocks suggest that the acoustic basement identified on seismic-reflection profile E (Fig. 8) is volcanic breccia with a phosphatized limestone matrix (Tables 1 to 4). The abundance of vesicles and vesicular palagonite in these volcanic rocks suggest eruption into shallow water.

The flat summit of Bikar Guyot is blanketed by a sediment cap approximately 15-m-thick. However, substrate outcrops must occur on the summit because a dredge bag was lost at station 12 in an attempt to sample ferromanganese nodules and a sediment gravity core at the same station returned with a bent barrel covered with a manganese-oxide stain.

Mn crusts collected in dredge haul D15 vary from 0 to 60-mm-thick, averaging 7 mm (Table 1). The cobalt content averages about 0.72 wt.% (Table 4) in the Bikar Guyot crusts and these crusts are the only samples that contain todorokite (Table 5). One Mn crust is also rich in apatite (Table 5).

RATAK GUYOT

Dredge hauls D17 and D18 were collected from the east flank of Ratak Guyot, located 120 km southwest of Taongi Atoll (Fig. 2). This guyot, is similar in morphology to Bikar Guyot. The west flank of Ratak Guyot, in water depths less than 3700 m, displays a 22^{o} average slope and in water less than 2300 m deep, the east flank has a 13^{o} average slope. Both slopes decrease with increasing water depth. Seismic-reflection profile F (3.5 kHz; Fig. 9) shows no evidence of sediment accumulation on the flanks, but an 80-in^3 seismic-reflection profile (Insert Fig. 9) denotes a possible talus deposit on the east flank that is approximately 160-m-thick. Rocks collected in dredge hauls D17 and D18 suggest that the acoustic basement is volcanic breccia with a phosphatized limestone matrix (Tables 1 to 4).

Volcanic rocks in D17 and D18 predominately consist of angular fragments of hawaiite and a few centimeter-size clasts of highly altered alkalai olivine basalt in a phosphatized biomicrite matrix (Tables 1 and 2). The pervasive oxidation of the hawaiite and the roundness of the altered basalt clasts suggest weathering and erosion of subaerially erupted lava, before its final deposition as submarine debris flows. Foraminifera found in the biomicrite are tentatively dated as Early Tertiary. Since no evidence exists for subaqueous eruption this foraminifera age may not be the eruption age of the lava.

Mn crusts collected in dredge hauls D17 and D18 vary from 0- to 100-mm-thick (Table 1). These represent the thickest Mn crusts recovered from the Marshall Islands. The average cobalt content of these crusts is 0.67 wt.% (Table 4). Carbonate apatite is abundant in most of the Ratak Guyot Mn crusts (Table 5).

A sedimentary blanket as much as 110-m-thick caps the relatively flat summit of Ratak Guyot (Fig. 9). Surficial sediment collected to a maximum subbottom depth of 40 cm (box cores BC1, BC2, and BC3) consists of nannofossil-foraminiferal ooze with a foraminifera-sand content of 70 percent. Preliminary paleontological analysis indicates that this surficial sediment is a mixture of late Pliocene to recent fauna.

Bottom camera photographs taken during box core operations BC2 and BC3 reveal long-crested nearly symmetrical ripples covering the pelagic sedimentary deposit (Fig. 10). The presence of rippled sandy surficial carbonate ooze on the summit of Ratak Guyot suggests that active current-induced sediment transport is removing the fine-grained nannofossil component of the sediment, similar to processes affecting other sediment-capped edifices

(Lonsdale and others, 1972; Johnson and Lonsdale, 1976). The terraces around the perimeter of the summit of Ratak Guyot are similar to erosional terraces described on Horizon Guyot in the Mid-Pacific Mountains (Lonsdale and others, 1972).

TAONGI ATOLL

One dredge haul (D20) was collected on the south flank of Taongi Atoll (Fig. 2). A seismic-reflection survey was not conducted prior to dredge haul D20, thus, the nature of the subbottom is unknown. Samples from dredge haul D20 consist of a bioclastic limestone with a thin Mn crust (Tables 1 and 2). The Mn-crusts from Taongi Atoll were not analyzed for chemical content because they were too thin to separate from the substrate.

SUMMARY

The geochemical analyses presented in Table 4 support the preliminary findings of Schwab and others (1985) that the Marshall Islands area is of economic interest for commercial exploitation of Mn crusts. The average chemical composition of bulk crusts is summarized in Table 6 and a correlation coefficient matrix for these bulk analyses is presented in Table 7. The mean cobalt concentration is 0.84 wt.% with a maximum value of 1.24 wt.%. In addition to the high average cobalt value, high concentrations of platinum (up to 0.93 ppm) were found in a few samples. However nickel and copper values are low. The high average values for Co and Pt strongly suggest that the Marshall Islands are a viable source area for these important metals and that detailed surveys of the Marshall Islands should be conducted in order to determine their true resource potential.

Although most of the Mn-crust samples collected on this cruise had average thicknesses less than the 4-cm minimum considered necessary for economic exploitation, the sample density is not adequate to evaluate the distribution of crust thicknesses. Mn crusts greater than 4-cm-thick were collected on Erikub Seamount (D6), Bikar Guyot (D15), and Ratak Guyot (D18), with an extremely thick 100 mm crust recovered from Ratak Guyot. Additional site surveys (sampling, bottom camera, and geophysical work) are necessary before the economic potential of Mn crusts in the Marshall Islands area can be determined.

REFERENCES

Chase, T.E., and Menard, H.W., 1973, Bathymetric atlas of the North Pacific Ocean: U.S. Naval Oceanographic Office, Washington, D.C., Publication No. 1301-2-3.

Craig, J.D., Andrews, J.E., and Meyland, M.A., 1982, Ferromanganese deposits in the Hawaiian Archipelago: Marine Geology, vol. 45, p. 127-133.

Cronan, D.S., 1977, Deep sea nodules: distribution and geochemistry, in Glasby, G.P., ed., Marine manganese deposits: Amsterdam, Elsevier Publ. Co., p. 11-44.

Frazer, J.Z., and Fisk, M.B., 1980, Availability of copper, nickel, cobalt, and manganese from ocean ferromanganese nodules (III): Series 80-16, Reference, Scripps Institute of Oceanography, 116 p.

Halbach, P., Hebisch, H., and Scherlag, C., 1981, Geochemical variations of ferromanganese nodules and crusts from different provinces of the Pacific Ocean and their genetic control: Chemical Geology, vol. 34, p. 3-17.

Halbach, P., and Manheim, F.T., 1984, Potential of cobalt and other metals in ferromanganese crusts on seamounts of the Central Pacific basin: Marine Mineralogy, vol. 4, p. 319-336.

Halbach, P., Manheim, F.T., and Otten, P., 1982, Co-rich ferromanganese nodules and crusts from different provinces of the Pacific Ocean and their genetic control: Chemical Geology, vol. 34, p. 3-17.

Halbach, P., Puteanus, D., and Manheim, F.T., 1984, Platinum concentrations in ferromanganese seamount crusts from the Central Pacific: Naturwissenschaften, vol. 71, p. 577-579.

Hein, J.R., Manheim, F.T., Schwab, W.C., Davis, A.S., Daniel, C.L., Bouse, R.M., Morgenson, L.A., Sliney, R.E., Clague, D., Tate, G.B., and Cacchione, D.A., 1985, Geological and geochemical data for seamounts and associated ferromanganese crusts in and near the Hawaiian, Johnston Island, and Palmyra Island Exclusive Economic Zones: U.S. Geological Survey Open-File Report 85-292, 129 p.

Hein, J.R., Morgenson, L.A., Clague, D.A., and Koski, R.A., 1986a, Cobalt-rich ferromanganese crusts from the Exclusive Economic Zone of the United States and nodules from the oceanic Pacific, IN Scholl, D., Grantz, A., and Vedder, J., eds., Geology and resource potential of the continental margins of western North America and adjacent ocean basins: American Association of Petroleum Geologists, Memoir (in press).

Hein, J.R., Manheim, F.T., Schwab, W.C., and Clague, D.A., 1986b, Cobalt-rich ferromanganese crusts from the central Pacific: Proceedings of the 18th Annual Offshore Technology Conference, Houstin (in press).

Johnson, D.A., and Lonsdale, P.F., 1976, Erosion and sedimentation around Mytilus Seamount, New England continental rise: Deep-Sea Research, vol. 23, p. 429-440.

Lonsdale, P.F., Normark, W.R., and Newman, W.A., 1972, Sedimentation and erosion on Horizon Guyot: Geological Society of America, Bulletin, vol. 83, p. 289-316.

Schwab, W.C., and Bailey, N.G., 1985, High-resoluton seismic-reflection data collected on R/V S.P. LEE: L9-84-CP, Marshall Islands to Hawaii: U.S. Geological Survey Open-File Report 85-24, 6 p.

Schwab, W.C., Davis, A.S., Haggerty, J.A., Ling, T.H., and Commeau, J.A., 1985, Geological reconnaissance and geochemical analysis of ferromanganese crusts of the Ratak Chain, Marshall Islands: U.S. Geological Survey Open-File Report 85-18, 6 p.

Toth, J.R., 1980, Deposition of submarine crusts rich in manganese and iron: Geological Society of America Bulletin, vol. 91 (part I), p. 44-54.

Table 1. Location and description of samples from the Marshall Islands, Cruise L9-84-CP.

Station No.	Sample[1] No.	Location	Latitude[2] °N	Longitude °E	Water Depth (m)	Sample Weight (kg)	Crust Description	Substrate Description
1	D1	Majuro Atoll	07°15.0' 07°14.4'	171°00.5' 171°00.9'	2250-2230	10	0 to 2 mm thick crusts (average <1 mm), smooth to granular and porous. About 90% broken from outcrop, 10% talus.	Dominantly pillow breccia: angular red-brown clasts in a pale-brown phosphatized limestone matrix. Volcanic clasts have plagioclase and pyroxene phenocrysts.
2	D2	Majuro Atoll	07°14.1' 07°14.2'	171°0.3' 171°0.2'	1480-1500	250	Few thin (<1 mm) crusts with irregular surface texture mirroring underlying substrate surface.	Fragments of poorly indurated limestone with whole and fragmented coral and shells.
3	D3	Majuro Atoll	07°15.5' 07°13.5'	170°59.1' 170°59.7'	2000-3100	1	No crust recovered.	One subangular dark-gray, aphyric basalt cobble with many plagioclase microlites, some of which show incipient trachytic texture. One rounded pale-brown bioclastic limestone.
4	D4	Erikub Seamount	08°44.8' 08°44.4'	169°44.3' 169°43.8'	3550	4	Three rocks have thin crusts (1 mm) and are smooth-abraded. Two crusts (variable thickness 1 to 6 mm) are botryoidal. Three rocks were broken from outcrop, one is from talus.	Volcanic breccia in pale-brown, phosphatized limestone matrix. Basalt clasts are angular to well-rounded (1 to 40 mm); some clasts are vesicular limestone, and red-brown altered palagonite clasts also occur. One well-rounded aphyric basalt cobble.
5	D5	Erikub Seamount	08°45.9' 08°46.0'	169°44.3' 169°44.5'	2500	0	No recovery - dredge bag coated with Mn-oxide.	-
5	D6	Erikub Seamount	08°45.3' 08°46.9'	169°47.5' 169°43.0'	2900	150	Two distinct crust groups: 30% of rocks with crusts 0 to 1 mm thick with smooth surface; 70% of rocks with crusts 10 to 40 mm thick, average 30 mm, with botryoidal or granular and porous surfaces. One fluted and polished crust, some crusts without substrates. about 70% broken from outcrop, 30% talus.	About 70% volcanic breccia with various amounts of basalt clasts in either phosphatized limestone or altered tuffaceous matrix. Other lithologies include calcareous phosphatic sandstone and basalt cobbles.
6	D7	Erikub Seamount	08°47.3'	169°43.8'	1500	0	No recovery	-
6	D8	Erikub Seamount	08°48.1'	169°46.3'	1750	0	No recovery	-
7	D9	Jemo Island	10°05.3' 10°04.9'	169°31.8' 169°30.3'	1000	0	No recovery	-

Table 1. continued

Station No.	Sample[1] No.	Location	Latitude[2] °N	Longitude °E	Water Depth (m)	Sample Weight (kg)	Crust Description	Substrate Description
8	D10	Jemo Island	10°05.1' 10°05.4'	169°36.6' 169°36.4'	1000-1680	2	Very thin (<1 mm) patina of Mn-oxide.	Three well-rounded paleo-brown to gray limestone cobbles. One was bioturbated, another has well preserved coral fragments.
9	D11	Jemo Island	11°02.2'	170°10.6' 170°10.0'	1500	0	No recovery	-
10	D12	Utirik Seamount	11°01.2' 11°01.0'	170°10.6' 170°10.0'	1575-2000	<1	One botryoidal crust 20 to 30 mm thick with an outer porous layer and inner massive layer.	No rocks recovered.
10	D13	Utirik Seamount	11°00.5' 11°00.5'	170°12.2' 170°11.9'	2000	1	Four crusts with mostly smooth to small-scale botryoidal surfaces. Crust thickness varies from 1 to 25 mm, avg. 15 mm. Two crusts have three distinct porous layers.	No rocks recovered.
10	D14	Utirik Seamount	11°0.3' 11°0.8'	170°13.8' 170°11.2'	1800	<1	Three crusts 5 to 25 mm thick, avg. 13 mm. One has botryoidal-porous surface, one has smooth and porous surface and the third is granular and porous. All have two distinct layers, an outer porous and inner massive layer.	No rocks recovered.
11	D15	Bikar Guyot	12°11.0' 12°10.7'	168°59.7' 168°58.3'	1300-1800	50	About 30% from outcrop, 70% from talus. Crusts are predominantly botryoidal or grsnular and porous; one has vugs filled with phosphorite. One is smooth. Crust thickness varies from 0 to 60 mm, averaging 7 mm.	Volcanic breccia with various amounts of basalt clasts in a phosphatized limestone matrix, bedded clastic limestone phosphatized to various degrees; basalt pebbles.
12	D16	Bikar Guyot	12°11.0'	168°57.2'	945	0	No recovery	-
12	GC1	Bikar Guyot	12°11.2'	168°52.2'	960	0	No recovery - barrel coated with Mn-oxide	-
13	D17	Ratak Guyot	13°54.3' 13°54.2'	167°37.6' 167°38.3'	1600	3	Five rocks broken from outcrop have crusts with botryoidal and porous surfaces. Three of these rocks have thin crusts 0 to 5 mm (2 mm ave.); one is manganese stained; of the two thicker 10 to 35 mm (20 mm ave.) layered crusts, one has no substrate and one has an inner porous layer with vugs filled with carbonate.	The four rocks with thin crusts are soft white limestone with Mn dendrites. Of the two with thicker crusts one has no substratum, the other rests on volcanic breccia.

Table 1. continued

Station No.	Sample[1] No.	Location	Latitude[2] °N	Longitude °E	Water Depth (m)	Sample Weight (kg)	Crust Description	Substrate Description
14	D18	Ratak Guyot	13°54.0' 13°54.0'	167°39.2' 167°38.5'	1600	50	60% broken from outcrop, 40% from talus, one nodule. Half the rocks have thin 0 to 6 mm (1.4 mm avg.) crusts, the other half have thick 10-100 mm (30 mm avg.) crusts and are typically layered (2 to 4 distinct layers). All are botryoidal and porous with some sbraded smooth areas.	40% volcanic breccia in phosphatized limestone matrix (some basalt clasts rimmed with Mn). 30% basalt: dark gray aphyric with phosphatized chalk layer; red-brown scoriaceous with thin limestone layers; highly altered basalt; basalt pebbles. 18% rounded, bioturbated, limestone pebbles. 20% no substrate.
15	D19	Ratak Guyot	13°55.3' 13°55.5'	167°31.9' 167°31.1'	1400	0	No recovery	-
15	BC1	Ratak Guyot	13°55.6'	167°27.7'	1380	-	-	5 cm of nannoplankton-foraminiferal ooze.
16	BC2	Ratak Guyot	13°55.7'	167°26.8'	1380	-	-	40 cm of nannoplankton-foraminiferal ooze. Bottom photo taken.
17	BC3	Ratak Guyot	13°54.8'	167°35.6'	1395	-	-	30 cm of nannoplankton-foraminiferal ooze. Bottom photo taken.
18	D20	Tanongi Atoll	14°32.5' 14°32.6'	169°0.2' 169°0.0'	1700-2000	1.5	About 60% of rocks have thin ferromanganese coatings (<1 mm) which mimics surface texture of substratum; 40% without crusts.	70% composed of coarse-grained bioclastic limestone: one rock with a layer of phosphorite between Mn crust and the limestone, one is burrowed, the rest are broken angular to subrounded pieces without manganese crusts. 15% well-rounded pebbles of coralline debris with no crust. 15% fine-grained bioclastic limestone.

[1] D = dredge haul, GC = gravity core, and BC = box core.
[2] Two latitudes and longitudes for some dredge hauls signify the beginning and end of contact with the sea floor.

Table 2. Minerals identified by X-ray diffraction in substrate rocks associated with ferromanganese crusts dredged from the Marshall Islands.

Sample[1]	Rock Type	Major	Moderate	Minor	Trace	Presence Uncertain
D1-2	Basalt	Phillipsite	Plagioclase	Carbonate-Apatite Smectite		
D1-4	Bulk breccia	Plagioclase	Smectite Pyroxene	Phillipsite		δ-MnO_2
D1-5-II	Breccia basalt clast	Plagioclase	Pyroxene			
D1-5-III	Breccia matrix	Carbonate-Apatite		Calcite Phillipsite		
D4-1-I	Thin layer between crust and breccia	Phillipsite	Smectite Carbonate-Apatite Plagioclase	Pyroxene		Barite Quartz
D4-1-II	Bulk breccia	Calcite Plagioclase	Smectite	Hematite Maghemite		Barite
D4-1-III	Breccia clast	Calcite Plagioclase	Smectite	Carbonate-Apatite K-feldspar Hematite Goethite Pyroxene Barite		
D4-1-IV	Breccia basalt clast	Plagioclase	Pyroxene			Smectite
D4-1-V	Breccia basalt clast	Plagioclase		Hematite Pyroxene Smectite		
D4-1-VI	Breccia matrix	Phillipsite		Smectite Plagioclase		
D4-3-II	Bulk breccia	Plagioclase		Hematite Pyroxene Phillipsite Smectite		
D4-3-III	Breccia basalt clast	Plagioclase	Smectite Pyroxene	Phillipsite Barite Hematite Goethite		
D6-2-IV	Breccia basalt clast	Plagioclase		Carbonate-Apatite Pyroxene		
D6-2-V	Breccia matrix	Carbonate-Apatite		Plagioclase	Smectite Phillipsite	
D6-2-VI	Breccia basalt clast	Plagioclase		Hematite Pyroxene		Barite

Table 2. continued

Sample[1]	Rock Type	Major	Moderate	Minor	Trace	Presence Uncertain
D6-4	Bulk breccia	Carbonate-Apatite			Smectite Plagioclase	
D6-7	Bulk breccia	Plagioclase Phillipsite	Carbonate-Apatite Calcite			
D6-8	Bulk breccia	Plagioclase	Carbonate-Apatite		Smectite Phillipsite	Calcite
D6-9	Bulk breccia	Carbonate-Apatite				
D6-10	Phosphatized siltstone	Carbonate-Apatite		Phillipsite	Barite	
D6-12	Bulk breccia	Carbonate-Apatite	Plagioclase	Smectite		
D6-13	Bulk breccia	Carbonate-Apatite	Phillipsite Plagioclase	Smectite		
D6-14	Bulk breccia	Carbonate-Apatite		Smectite Phillipsite		
D6-15c	Phosphatized limestone	Carbonate-Apatite		Plagioclase Phillipsite		
D6-19	Bulk breccia	Carbonate-Apatite		Barite	Quartz Plagioclase	Smectite
D6-20	Bulk breccia	Carbonate-Apatite	Barite	Plagioclase	Smectite	Mn-calcite
D6-21	Bulk breccia	Carbonate-Apatite		Smectite Barite		
D6-22	Phosphatized limestone with basalt clasts	Carbonate-Apatite Plagioclase	Calcite	Smectite Barite Pyroxene Phillipsite		
D6-23	Bulk breccia	Plagioclase	Smectite Pyroxene Carbonate-Apatite	Calcite Phillipsite		δ-MnO_2
D6-25	Phosphatized limestone	Carbonate-Apatite		Phillipsite		
D10-1	Limestone	Calcite				
D15-1e	Phosphatized limestone	Carbonate-Apatite	Calcite	Quartz Phillipsite		
D15-2	Phosphatized hyaloclastite	Carbonate-Apatite	Smectite	Phillipsite		
D15-3-III	Bulk breccia	Carbonate-Apatite Phillipsite		Smectite	Plagioclase	
D15-3-IV	Phosphatized limestone	Carbonate-Apatite Calcite				

Table 2. continued

Sample[1]	Rock Type	Major	Moderate	Minor	Trace	Presence Uncertain
D15-4	Phosphatized limestone	Carbonate-Apatite			Calcite	
D15-6	Phosphatized limestone	Carbonate-Apatite			Calcite	
D17-2	Phosphatized limestone	Carbonate-Apatite				
D18-1-IV	Bulk breccia	Plagioclase	Carbonate-Apatite Pyroxene	Calcite Smectite	Mixed layer clay Pyrolusite Barite	
D18-1-V	Radial crystals in vugs	Phillipsite Plagioclase	Carbonate-Apatite Chabazite	Analcime Pyroxene		Smectite
D18-2	Bulk breccia	Carbonate-Apatite		Smectite Calcite	Phillipsite	
D18-3	Phosphatized limestone matrix of breccia	Carbonate-Apatite Calcite				
D18-9	Bulk breccia	Plagioclase	Maghemite	Smectite Carbonate-Apatite Phillipsite Pyroxene	Quartz Calcite	
D18-10b	Phosphatized limestone	Carbonate-Apatite		Barite		
D18-11	Basalt	Pyroxene Plagioclase		Smectite		
D20-1	Limestone	Calcite		Aragonite		

[1]The first number indicates the dredge haul number, the second number indicates an individual rock in the dredge haul, and the Roman numeral indicates a subsample of this rock.

Table 3. Chemical composition of rocks dredged from the Marshall Islands; major oxides in weight percent. Pt and Pd in ppm. Totals based on loss on ignition (LOI).

	D1-1[1]	D1-8	D2-8A	D4-1	D4-8	D4-4	D6-1	D6-4	D10-1B
SiO_2	40.0	43.0	0.49	42.1	43.6	42.0	28.7	12.6	1.07
Al_2O_3	14.2	14.4	0.16	14.4	15.9	15.0	8.23	3.83	0.86
Fe_2O_3	11.83	10.19	<0.04	13.16	13.00	12.14	9.66*	3.48*	0.073
FeO	8.49	4.69	<0.02	0.76	2.16	2.22	—	—	0.06
MgO	2.90	3.58	1.52	2.16	2.59	2.55	1.34	0.99	0.93
CaO	7.57	8.86	52.7	6.40	6.07	6.47	24.2	41.2	54.5
Na_2O	3.15	2.87	0.31	3.00	2.87	2.81	2.46	1.24	<0.15
K_2O	1.24	1.07	<0.02	2.39	1.85	1.76	1.83	0.77	0.02
TiO_2	4.06	4.00	<0.02	2.78	3.62	3.24	1.25	0.65	0.05
P_2O_5	1.04	1.18	0.06	1.08	0.64	0.66	14.0	25.3	0.15
MnO	0.26	0.29	<0.02	0.21	0.21	0.20	1.75	0.28	0.08
LOI 900 °C	9.92	5.91	45.0	11.7	7.29	10.5	8.70	6.84	43.9
Total	99.66	99.54	100.30	100.09	99.80	99.55	97.12	97.18	101.21
H_2O^+	2.35	2.24	0.70	2.74	2.84	1.92	2.59	2.61	0.11
CO_2	0.47	0.19	42.2	1.40	0.14	0.31	3.30	4.54	42.9
Pd	<0.001†	—	<0.001	—	—	<0.001	—	—	<0.001
Pt	0.011	—	<0.010	—	—	<0.010	—	—	<0.010
Lithology	pillow breccia	pillow breccia	limestone	zeolitized volcanic breccia	zeolitized volcanic breccia	zeolitized volcanic breccia	volcanic breccia in phosphatized limestone matrix	volcanic breccia in phosphatized limestone matrix	limestone

	D15-1E	D15-2	D15-3	D15-4	D17-2	D17-4	D17-6	D18-3	D18-10B
SiO_2	8.58	21.0	17.2	2.61	0.88	0.55	20.5	8.84	—
Al_2O_3	2.50	5.19	4.64	0.86	0.14	0.12	9.10	3.85	—
Fe_2O_3	5.68*	9.50	8.54*	2.18*	0.002	0.15*	18.4*	8.45*	—
FeO	—	<0.02	—	—	0.07	—	—	—	—
MgO	1.19	4.39	2.21	0.71	0.88	0.45	3.99	0.75	—
CaO	42.2	25.7	29.7	47.8	52.7	53.1	14.6	42.4	—
Na_2O	1.26	1.63	1.57	1.10	0.88	0.70	1.80	1.21	—
K_2O	0.59	1.01	1.21	0.09	<0.02	<0.02	1.04	0.51	—
TiO_2	0.40	1.54	1.45	0.32	0.07	0.07	3.00	0.59	—
P_2O_5	24.5	15.8	14.9	26.1	32.4	28.4	10.0	18.0	—
MnO	0.60	0.30	0.51	1.57	0.13	0.25	2.71	0.92	—
LOI 900 °C	9.08	11.7	15.8	13.4	8.39	18.8	11.7	17.1	—
Total	96.48	97.77	97.23	96.24	96.05	97.60	96.84	97.62	—
H_2O^+	3.63	4.21	3.34	2.23	2.07	1.28	9.58	2.26	1.76
CO_2	6.59	2.70	7.06	9.36	6.42	16.4	2.17	13.7	5.55
Pd	—	0.003	—	—	—	—	—	—	0.001
Pt	—	0.032	—	—	—	—	—	—	0.044
Lithology	phosphatized limestone	altered basalt clasts in phosphatized limestone	altered basalt clasts in phosphatized limestone	phosphatized limestone	phosphatized limestone	phosphatized limestone	altered basalt clasts in phosphatized limestone	phosphatized limestone	phosphatized limestone

1) The first number of the sample number indicates the dredge haul, the second number indicates an individual rock in dredge haul, and the letter indicates a subsample of this rock.

— means no data.

* means total iron reported as Fe_2O_3.

† Rh is <0.001 ppm for all samples analyzed.

Major oxides analyzed by X-ray spectroscopy, U.S. Geological Survey analytical laboratory, Denver, K. Stewart provided analytical expertise. H_2O^+, CO_2 analyzed at U.S. Geological Survey analytical laboratory, Menlo Park, N. Elsheimer provided analytical expertise. Platinum group elements analyzed in Denver laboratory, R. Mendes, A. Love, and C. Gent provided analytical expertise.

Table 4. Chemical composition of ferromanganese crusts dredged from the Marshall Islands.

	D1-1	D1-3	D1-8	D4-3	D4-4	D6-1-A	D6-1-B	D6-1-C
Si (wt. %)	2.43	2.57	1.50	15.4	5.56	1.59	1.18	0.87
Al	0.57	0.49	0.28	5.30	1.66	0.38	0.32	0.41
Fe	11.5	13.2	10.6	11.9	13.0	11.30	11.6	7.6
Mg	0.88	0.86	0.94	1.24	1.07	0.96	0.76	0.83
Ca	2.25	2.19	2.22	3.3	2.35	2.22	8.7	16.2
Na	1.46	1.43	1.57	1.97	1.71	1.30	1.30	1.23
K	0.49	0.44	0.34	1.79	0.77	0.41	0.31	0.30
Ti	0.80	0.79	0.86	1.49	1.17	1.08	0.69	0.52
P	0.34	0.37	0.31	0.38	0.34	0.25	2.74	5.1
Mn	20.7	20.5	23.1	5.80	17.2	21.3	17.2	14.8
H_2O^-	27.0	25.5	27.0	11.1	19.6	27.6	20.7	14.3
H_2O^+	5.4	6.6	6.0	3.5	—	5.3	4.8	5.0
CO_2	0.61	0.59	0.53	0.71	0.41	0.66	1.58	3.7
As (ppm)	205	230	200	87	180	180	160	93
Ba	830	890	860	420	930	1400	1700	1600
Cd	4.1	3.7	1.92	0.53	2.55	4.1	2.30	2.20
Co	10,000	8400	12,400	1200	7200	9000	2600	2200
Cr	3.5	6.0	2.00	70	46	6.5	5.5	6.0
Cu	200	220	210	220	470	700	800	1100
Mo	310	320	370	73	280	350	300	270
Ni	4100	3800	4900	790	3000	5600	4200	4600
Pb	1200	1200	1200	390	1100	1300	1100	730
Sr	1100	1200	1100	650	1000	1100	1400	1300
V	470	530	460	360	450	410	450	340
Zn	600	570	620	290	490	690	600	720
Y	140	160	140	67	130	130	630	280
Ce	730	730	770	270	860	1100	1100	770
Sampled Interval†	bulk (0-2 mm)	bulk (0-2 mm)	bulk (0-2 mm)	bulk* (0-2 mm)	bulk** (0-5 mm)	(0-10 mm)	(10-20 mm)	Mn phosphorite cement

Table 4. continued

	D6-2-A	D6-2-B	D6-2-C	D6-2-D	D6-4A	D6-6-A	D6-6-B	D6-6-C
Si (wt. %)	2.90	4.35	2.34	1.28	2.24	1.54	3.18	1.96
Al	0.52	1.19	0.58	0.28	0.34	0.19	0.77	0.48
Fe	14.1	15.8	14.7	10.6	15.0	12.7	14.6	15.1
Mg	0.83	0.84	0.90	0.77	0.88	0.83	0.83	0.81
Ca	1.93	2.12	2.11	8.0	2.03	2.18	2.12	2.27
Na	1.36	1.38	1.28	1.37	1.71	1.35	1.39	1.18
K	0.35	0.51	0.37	0.30	0.32	0.36	0.47	0.35
Ti	0.84	1.10	1.08	0.72	0.68	0.65	1.04	1.05
P	0.33	0.43	0.33	2.54	0.37	0.34	0.29	0.34
Mn	19.7	16.8	20.8	19.4	19.4	22.3	20.3	20.5
H_2O^-	25.2	22.2	21.7	19.6	25.5	26.4	22.1	23.7
H_2O^+	5.6	6.5	6.6	5.8	5.6	5.5	6.4	6.1
CO_2	0.50	0.51	0.47	1.32	0.43	0.49	0.43	0.48
As (ppm)	225	170	210	160	260	250	195	220
Ba	1200	1400	1800	1500	920	970	1500	2100
Cd	2.98	2.35	3.4	2.68	2.65	3.25	2.70	2.35
Co	5900	4100	6100	3800	5300	6600	5200	4400
Cr	25	13	6.8	4.5	2.50	2.50	17	3.5
Cu	410	700	950	810	420	310	840	1200
Mo	380	230	420	460	370	530	360	460
Ni	3600	3400	4100	4400	3000	4000	3800	3700
Pb	1300	1100	1300	1100	1200	1400	1100	1100
Sr	1300	1200	1400	1500	1200	1300	1300	1500
V	570	440	590	500	570	620	510	630
Zn	550	610	760	620	490	500	660	830
Y	140	150	120	220	150	160	130	120
Ce	630	740	910	1100	660	550	730	1000
Sampled Interval[†]	surface botryoids (0-7 mm)	(7-15 mm)	(20-40 mm)	(40-60 mm)	bulk (0-5 mm)	(0-10 mm)	(10-25 mm)	(25-35 mm)

Table 4. continued

	D6-13-A	D6-13-B	D6-13-C	D12-1-A	D12-1-B	D12-1-C	D13-1-A	D13-1-B
Si (wt. %)	1.96	3.46	2.29	2.10	3.23	1.10	1.45	0.97
Al	0.30	0.78	0.57	0.41	0.88	0.24	0.21	0.12
Fe	13.4	14.3	14.5	13.4	14.3	11.7	10.6	11.5
Mg	0.83	0.80	0.80	0.88	0.90	0.87	0.91	0.96
Ca	1.99	1.78	1.91	2.12	2.45	2.38	1.95	2.45
Na	1.36	1.31	1.26	1.36	1.33	1.37	1.48	1.48
K	0.31	0.44	0.35	0.39	0.49	0.41	0.35	0.39
Ti	0.75	0.98	0.99	0.74	1.01	0.76	0.91	0.92
P	0.32	0.25	0.26	0.36	0.31	0.27	0.27	0.28
Mn	20.4	17.8	18.4	21.5	19.9	24.1	22.5	25.6
H_2O^-	26.8	26.2	26.5	25.1	21.2	25.0	26.7	20.8
H_2O^+	5.4	5.5	5.6	6.2	6.7	6.5	4.1	6.5
CO_2	0.48	0.41	0.41	0.50	0.95	0.55	0.47	0.43
As (ppm)	240	180	210	250	200	220	190	200
Ba	1100	1300	1800	1000	1500	1700	990	1700
Cd	2.8	2.7	2.3	3.0	3.1	3.25	4.3	4.3
Co	6200	4700	5000	7600	5400	7100	13,300	9200
Cr	8.3	16	6.8	3.5	9.0	1.00	4.8	5.3
Cu	530	870	1300	490	760	850	280	870
Mo	430	270	370	460	350	650	420	680
Ni	3600	3900	3600	4000	4700	5300	4700	5900
Pb	1300	990	1000	1500	1300	1200	1500	1400
Sr	1200	1100	1200	1300	1200	1300	1200	1400
V	550	430	580	590	480	600	470	600
Zn	530	530	650	580	660	710	590	830
Y	150	110	86	150	110	97	140	110
Ce	610	740	900	670	800	880	860	1100
Pd	0.0016	0.0012	0.0020					
Pt	0.12	0.28	0.63					
Rh	0.0036	0.011	0.039					
Sampled Interval†	porous surface (0-5 mm)	(5-25 mm)	(25-45 mm)	(0-5 mm)	(5-15 mm)	(15-25 mm)	(0-8 mm)	(10-20 mm)

Table 4. continued

	D13-1-C	D13-2-A	D13-2-B	D13-2-C	D14-1-A	D14-1-B	D15-1e-A	D15-2-A
Si (wt. %)	1.07	1.36	1.02	0.86	1.78	1.08	1.40	1.87
Al	0.20	0.25	0.18	0.18	0.27	0.23	0.39	0.29
Fe	12.2	10.7	11.0	10.4	11.3	11.2	11.1	12.9
Mg	0.84	0.89	0.95	0.84	0.82	0.77	0.96	0.82
Ca	2.22	2.03	2.17	2.32	1.92	4.1	2.04	1.99
Na	1.46	1.47	1.49	1.37	1.34	1.28	1.83	1.31
K	0.31	0.39	0.45	0.38	0.34	0.30	0.38	0.35
Ti	0.79	1.04	1.16	0.80	0.93	0.79	0.74	0.66
P	0.27	0.27	0.21	0.28	0.28	1.05	0.32	0.35
Mn	21.5	22.4	25.0	22.3	20.3	19.4	21.9	20.6
H_2O^-	27.4	27.6	23.1	30.0	28.9	28.1	26.6	28.1
H_2O^+	5.0	6.3	6.7	5.4	5.4	5.4	5.5	5.2
CO_2	0.41	0.47	0.37	0.38	0.44	0.70	0.37	0.32
As (ppm)	190	190	180	170	210	180	220	250
Ba	1800	930	1700	1900	990	1800	1000	830
Cd	3.4	4.1	4.7	3.6	3.5	2.7	3.6	3.1
Co	4100	14,200	10,200	5900	11,100	4800	9800	7400
Cr	3.3	2.00	2.00	2.50	6.8	6.3	3.5	4.0
Cu	1000	240	870	960	260	940	720	220
Mo	390	330	370	410	330	400	460	420
Ni	5000	4000	5800	5000	3900	4200	4600	3600
Pb	1300	1500	1700	1700	1400	1300	1600	1500
Sr	1300	1100	1200	1200	1100	1300	1100	1100
V	500	420	410	440	460	510	510	530
Zn	640	550	740	660	540	620	560	520
Y	150	140	110	160	140	360	110	150
Ce	1300	1000	1400	1500	880	1300	600	590
Pd					0.0012	0.0016		
Pt					0.21	0.93		
Rh					0.013	0.027		
Sampled Interval†	(20-25 mm)	(0-3 mm)	(5-16 mm)	(17-20 mm)	porous surface (0-5 mm)	(20-25 mm)	bulk (0-5 mm)	(0-5 mm)

Table 4. continued

	D15-2-B	D15-2-C	D15-3-A	D15-3-B	D15-4-A	D15-9	D17-2-A	D17-6
Si (wt. %)	2.99	1.04	1.92	1.54	1.54	1.96	3.46	2.95
Al	0.81	0.28	0.61	0.41	0.31	0.35	0.50	0.46
Fe	14.2	11.2	10.9	13.6	12.0	12.2	13.1	12.5
Mg	0.88	0.92	1.18	0.94	0.91	0.84	0.87	0.82
Ca	2.04	2.33	2.22	3.9	2.16	1.99	2.35	1.86
Na	1.35	1.38	1.50	1.45	1.52	1.37	1.57	1.38
K	0.49	0.40	0.40	0.34	0.38	0.35	0.37	0.37
Ti	0.97	0.77	0.96	0.91	0.81	0.84	0.59	0.71
P	0.33	0.31	0.41	1.04	0.34	0.33	0.52	0.32
Mn	18.9	22.9	20.9	20.0	20.9	20.2	19.0	19.5
H_2O^-	25.0	27.4	25.3	20.8	28.2	27.7	25.3	27.0
H_2O^+	5.5	5.4	5.3	6.5	5.3	5.7	5.1	5.2
CO_2	0.41	0.39	0.51	0.77	0.44	0.35	0.43	0.37
As (ppm)	210	205	170	200	220	230	260	240
Ba	1400	1700	1300	1700	1100	1100	915	1100
Cd	2.15	3.3	4.8	3.2	3.05	3.3	2.55	2.9
Co	4500	6200	7900	5300	8600	7800	6000	7200
Cr	7.0	3.0	16	11	4.0	6.8	3.0	7.8
Cu	950	1700	1200	1300	450	450	290	440
Mo	310	590	370	440	410	400	420	410
Ni	3700	5600	6900	4900	4000	4100	3100	3800
Pb	1200	1100	1300	1200	1400	1500	1600	1500
Sr	1200	1300	1100	1400	1200	1200	1200	1200
V	480	550	450	610	510	490	570	500
Zn	560	750	800	770	580	530	480	490
Y	140	97	110	310	140	150	140	130
Ce	770	810	830	830	760	730	570	650
Pd						0.0012		0.0012
Pt						0.31		0.20
Rh						0.011		0.0041
Sampled Interval†	(5-25 mm)	(25-55 mm)	(0-5 mm)	(5-15 mm)	bulk (0-10 mm)	bulk (0-30 mm)	bulk (0-5 mm)	bulk (0-30 mm)

Table 4. continued

	D17-6#	D18-1-A	D18-1-B	D18-1-C	D18-3-A	D18-3-B	D18-7-A	D18-7-B
Si (wt. %)	1.15	1.92	4.11	1.26	2.66	0.95	1.92	1.21
Al	0.29	0.37	0.95	0.36	0.39	0.21	0.34	0.24
Fe	10.7	12.4	15.3	10.6	13.0	9.0	13.6	11.7
Mg	0.85	0.84	0.83	0.73	0.81	0.79	0.81	0.86
Ca	2.07	1.92	2.30	12.2	1.87	6.9	2.00	2.11
Na	1.33	1.42	1.45	1.29	1.43	1.39	1.36	1.35
K	0.39	0.35	0.49	0.26	0.33	0.31	0.38	0.38
Ti	0.87	0.98	0.98	0.70	0.72	0.60	0.77	0.77
P	0.32	0.32	0.55	4.2	0.36	2.18	0.36	0.30
Mn	20.7	20.0	17.0	15.7	18.5	19.3	19.9	22.1
H_2O^-	31.4	27.9	22.1	15.5	27.7	24.9	27.5	27.9
H_2O^+	5.1	6.0	6.4	5.6	4.9	5.0	5.2	5.3
CO_2	0.32	0.48	0.49	2.08	0.42	1.1	0.41	0.38
As (ppm)	190	200	205	150	260	160	250	220
Ba	1400	920	1300	1300	910	1400	1000	1200
Cd	3.25	3.3	2.30	2.32	2.7	3.4	2.70	2.75
Co	7900	12,400	4600	3600	7700	3900	8000	6900
Cr	21	10	17	7.0	5.3	2.3	6.5	1.00
Cu	680	160	650	990	220	930	280	640
Mo	370	310	270	350	380	490	410	500
Ni	4700	3400	3200	3400	3000	5000	3200	4500
Pb	1500	1600	1400	860	1500	1100	1600	1500
Sr	1100	1100	1200	1500	1200	1300	1200	1300
V	430	460	490	480	520	460	540	510
Zn	640	530	520	600	430	650	500	550
Y	140	140	240	230	150	250	160	120
Ce	1000	1100	920	550	720	730	790	760
Pd					0.0010	0.0016		
Pt					0.13	0.33		
Rh					0.0036	0.019		
Sampled Interval†	bulk (0-30 mm)	knobby surface (0-7 mm)	porous (10-25 mm)	massive (25-60 mm)	(0-5 mm)	(5-30 mm)	knobby surface (0-5 mm)	(5-15 mm)

Table 4. continued

	D18-7-C	D18-7-D	D18-10b-A	D18-11
Si (wt. %)	4.02	0.90	2.20	2.76
Al	1.28	0.27	0.38	0.51
Fe	14.1	8.9	12.5	13.6
Mg	0.94	0.79	0.92	0.81
Ca	2.19	8.4	3.2	1.97
Na	1.20	1.21	1.37	1.34
K	0.64	0.36	0.35	0.40
Ti	0.82	0.60	0.77	0.83
P	0.37	2.62	0.77	0.35
Mn	17.1	19.3	19.4	19.0
H_2O^-	25.4	22.6	25.5	26.7
H_2O^+	4.8	5.7	6.0	5.3
CO_2	0.35	1.38	0.56	0.33
As (ppm)	210	150	230	235
Ba	1200	1400	1000	930
Cd	1.58	2.85	2.75	2.40
Co	3900	3700	8700	9100
Cr	11	<1.0	36	13
Cu	820	930	220	200
Mo	300	440	310	320
Ni	3200	4900	3400	3000
Pb	1000	1200	1500	1600
Sr	1200	1300	1200	1200
V	480	440	510	480
Zn	520	650	520	440
Y	160	190	150	150
Ce	610	850	750	810
Sampled Interval†	(25-40 mm)	(40-45 mm)	bulk (0-2 mm)	bulk (0-6 mm)

Major and minor elements determined by Induction Coupled Plasma Emission Spectroscopy on samples dried at 110°C. Pt, Pd, and Rh determined by fire assay. H. Kirschenbaum and Z. Brown provided analytical expertise.

Sample numbers which are identical except for the suffixes -A, -B, -C, and -D represent different sample intervals from the same crust.

* significant contamination by substrate rock.
** slight contamination by substrate rock.
† Measured from outer surface of crust; bulk means the entire crust thickness was sampled and analyzed.
# Different bulk sections through crust D17-6 were sampled and analyzed.

Table 5. Mineral content (in percent) of ferromanganese crusts, Marshall Islands.

Sample	δMnO_2	Todorokite	Carbonate-Apatite	Plagioclase	Quartz	Calcite	Other	Comments
D1-2	100.0							bulk† (0-2 mm)
D1-5	95.8		4.2	trace				bulk (0-2 mm)
D4-2	100.0							bulk (0-6 mm)
D4-3	95.5			3.9	0.6			bulk (0-2 mm)
D6-1	100.0							bulk (0-30 mm)
D6-2-III	100.0							0-7 mm
D6-2-I	98.7				0.6		0.7 clinoptilolite	10-25 mm
D6-2-II	100.0							25-50 mm
D6-4	99.0				0.3	0.7		bulk (0-5 mm)
D6-6-I	100.0							0-10 mm
D6-6-II	100.0							10-35 mm
D6-7	100.0							bulk (0-2 mm)
D6-8-I	98.7					1.3		0-10 mm
D6-8-II	96.9			1.5	0.5		1.1 goethite	10-25 mm
D6-10	96.9				0.3		2.8 phillipsite	0-5 mm
D6-11-I	99.1				0.4		0.5 natrojarosite	0-5 mm
D6-11-II	99.2						0.8 goethite manganosite?	25-30 mm
D6-12-I	100.0							0-10 mm
D6-12-II	100.0							20-25 mm
D6-12-III	100.0							40-50 mm
D6-13-I	99.6				0.4			0-7 mm
D6-13-II	94.8		1.3	2.2	0.5	1.2		10-30 mm
D6-13-III	98.9				0.3		0.8 goethite	35-45 mm
D6-14	100.0							bulk (0-1 mm)
D6-15c	99.5				0.5			bulk (0-1 mm)
D6-19	99.4				0.6			bulk (0-9 mm)
D6-20	100.0							0-10 mm
D6-21-I	99.6				0.4			0-5 mm
D6-21-II	95.3				0.8		3.9 phillipsite	5-15 mm
D6-23	97.5			1.5	1.0			0-10 mm
D12-1-I	100.0				trace			0-5 mm
D12-1-II	99.1				0.9			5-15 mm

Table 5. continued

Sample	δMnO_2	Todorokite	Carbonate-Apatite	Plagioclase	Quartz	Calcite	Other	Comments
D12-1-III	100.0							20-25 mm
D13-1	100.0							bulk (0-25 mm)
D13-2-I	100.0							porous 0-3 mm
D13-2-II	100.0							5-13 mm
D13-2-III	100.0							17-20 mm
D13-3	100.0							bulk (0-25 mm)
D13-4	98.5		1.5					bulk (0-10 mm)
D14-1	100.0							bulk (0-25 mm)
D14-2	100.0							bulk (0-15 mm)
D14-3	100.0							bulk (0-15 mm)
D15-1e	94.2				0.5		5.3 phillipsite	bulk (0-5 mm)
D15-2-I	99.3				0.7			0-5 mm
D15-2-II	100.0		trace					2-25 mm
D15-2-III	100.0							25-60 mm
D15-3-I	92.2	6.0					1.8 birnessite	granular black from side of rock (0-3 mm)
D15-3-II	89.5		9.1				1.4 goethite	porous layer in crust (10-15 mm)
D15-4	100.0		trace					bulk (0-10 mm)
D15-6	100.0							bulk (0-3 mm)
D15-9	97.2	2.8						bulk (0-30 mm)
D17-2	90.4		6.0	1.0	2.6			bulk (0-5 mm)
D17-5	99.7				0.3			bulk (0-35 mm)
D17-6	99.5				0.5			bulk (0-30 mm)
D18-1-I	99.3				0.7			0-7 mm
D18-1-II	98.0				0.7		1.3 goethite	porous 10-25 mm
D18-1-III	91.8		7.2				1.0 goethite	massive 40-60 mm
D18-2-I	99.3				0.7			0-10 mm
D18-2-II	99.4				0.6			porous 10-20 mm
D18-2-III	90.7		9.3					massive 50-70 mm
D18-2-IV	97.0			1.0		0.9	1.1 goethite	porous crust on underside of rock
D18-3-I	99.8				0.2			0-3 mm
D18-3-II	90.3		9.7					massive 3-10 mm
D18-3-III	98.9				0.5		0.6 smectite	porous 10-25 mm
D18-4-I	99.8				0.2			0-7 mm

Table 5. continued

Sample	δMnO_2	Todorokite	Carbonate-Apatite	Plagioclase	Quartz	Calcite	Other	Comments
D18-4-II	100.0							porous 20-35 mm
D18-6	93.6		6.4					bulk (0-15 mm)
D18-7-I	99.2				0.8			0-5 mm
D18-7-II	100.0							5-15 mm
D18-7-III	99.5				0.5			25-40 mm
D18-7-IV	95.7		4.3					40-50 mm
D18-9	98.3		1.1			0.6		bulk (0-5 mm)
D18-10b	90.3		9.7					bulk (0-1 mm)
D18-11	99.3				0.7			bulk (0-6 mm)
D18-12	97.5		1.2	0.8	0.5			bulk (0-20 mm)

Percentages were determined by using the following weighting factors relative to quartz set as 1: δ-MnO_2 75, plagioclase 2.8, apatite 3.1, calcite 1.65. We determined the δ-MnO_2 weighting factor by mixing known amounts of a pure δ-MnO_2 crust and quartz; other weighting factors are from Cook et al. (1975). The limit of detection for each mineral falls between 0.2 and 1.0 percent.

Sample numbers which are identical except for the suffixes -I, -II, -III, and -IV represent different sample intervals from the same crust.

Intervals listed in millimeters are measured from the outer surface of the crust.

† Bulk means a representative section through the entire crust was analyzed.

Table 6. Statistics for 12 Marshall Islands bulk crusts.

Element	Mean	St. Dev.	Median	Maximum	Minimum
Si (wt. %)	2.18	0.70	2.22	3.46	1.15
Al	0.41	0.10	0.39	0.57	0.28
Fe	12.3	1.28	12.4	15.0	10.6
Mg	0.88	0.05	0.88	0.96	0.81
Ca	2.19	0.35	2.12	3.20	1.86
Na	1.49	0.16	1.45	1.83	1.33
K	0.38	0.05	0.3.8	0.49	0.32
Ti	0.77	0.08	0.80	0.87	0.59
P	0.39	0.13	0.34	0.77	0.31
Mn	20.4	1.23	20.4	23.1	19.0
H_2O^-	27.0	1.68	26.9	31.4	25.3
H_2O^+	5.57	0.45	5.45	6.60	5.10
CO_2	0.44	0.10	0.43	0.61	0.32
As (ppm)	227	21.6	230	260	190
Ba	1,003	156	965	1,400	830
Cd	3.01	0.61	2.98	4.10	1.92
Co	8433	1872	8500	12,400	5,300
Cr	9.1	10.1	5.0	36.0	2.0
Cu	375	184	355	720	200
Mo	373	49.4	370	460	310
Ni	3875	657	3,900	4,900	3,000
Pb	1,417	170	1,500	1,600	1,200
Sr	1,167	49.2	1,200	1,200	1,100
V	503	41.4	505	570	430
Zn	543	61.7	545	640	440
Y	142	12.7	140	160	110
Ce	730	111	730	1,000	570

Table 7. Correlation coefficient matrix for Marshall Islands crusts (bulk samples). Correlations at greater than 95% confidence level are boldface.

	Si	Na	H_2O^+	H_2O^-	CO_2	Ca	Fe	K	Mg	P	As	Ba	Cd
Na	-.196												
H_2O^+	-.082	.005											
H_2O^-	**-.633**	-.357	-.438										
CO_2	.137	.034	**.637**	-.469									
Ca	.050	-.138	.346	-.332	.569								
Fe	**.628**	.046	.095	**-.607**	-.026	-.032							
K	.173	-.256	.025	.094	.402	-.076	-.202						
Mg	-.527	**.685**	.275	-.172	.392	.421	-.418	-.193					
P	.296	-.159	.207	-.449	.356	**.927**	.233	-.208	.204				
As	**.726**	.220	-.045	**-.710**	-.127	.000	**.870**	-.364	-.272	.317			
Ba	-.470	-.361	-.424	**.830**	**-.633**	-.175	-.345	-.196	-.241	-.135	-.342		
Cd	-.120	-.013	.076	.170	.209	-.108	-.201	**.712**	-.019	-.199	-.268	.114	
Co	-.463	.007	.312	.149	.349	.118	**-.701**	.269	.475	-.189	**-.739**	-.246	-.018
Cr	-.107	-.546	.086	.162	.012	**.687**	-.065	-.115	-.056	**.705**	-.163	.401	-.086
Cu	-.565	.327	-.420	.569	**-.661**	-.402	-.324	-.241	.147	-.361	-.194	**.724**	.279
Mn	**-.723**	.375	.282	.298	.220	-.129	**-.755**	.041	**.662**	-.442	**-.718**	-.038	.071
Mo	-.190	.555	-.432	.142	-.565	-.423	-.215	-.425	.254	-.321	.166	.304	-.054
Ni	**-.759**	.100	.087	**.606**	.014	-.184	**-.914**	.116	.432	-.463	**-.851**	.337	.250
Pb	.127	-.133	-.542	.156	**-.697**	.011	-.074	-.213	-.191	.228	.190	.439	-.128
Sr	**.592**	-.270	.110	-.461	-.095	.105	**.781**	-.294	-.461	.367	**.785**	-.089	-.245
Ti	**-.655**	-.457	.236	**.621**	.001	-.084	-.538	.209	-.017	-.333	**-.810**	.306	.111
V	.547	.487	.128	**-.762**	.133	.127	**.748**	-.284	.082	.344	**.892**	-.434	-.107
Zn	**-.730**	.029	.192	**.584**	.319	.036	**-.781**	.292	.450	-.296	**-.865**	.276	.362
Al	**.781**	-.170	-.056	-.466	.277	-.013	.318	**.691**	-.405	.094	.319	-.513	.359
Y	.286	-.548	.475	-.183	.333	.250	.516	.042	-.441	.272	.205	-.173	-.144
Ce	-.523	**-.610**	-.035	**.777**	-.143	.005	-.368	.154	-.238	-.147	**-.694**	**.580**	-.001

	Co	Cr	Cu	Mn	Mo	Ni	Pb	Sr	Ti	V	Zn	Al	Y
Cr	-.016												
Cu	-.217	-.046											
Mn	.777	-.323	.213										
Mo	-.199	-.448	**.709**	.226									
Ni	**.655**	-.128	.436	**.888**	.274								
Pb	-.219	.343	.396	-.370	.439	-.159							
Sr	**-.628**	.117	-.311	**-.744**	-.075	**-.787**	.181						
Ti	**.653**	.234	.012	.501	-.366	**.588**	-.195	-.389					
V	**-.643**	-.274	-.138	-.466	.228	**-.684**	-.019	**.625**	**-.848**				
Zn	.543	-.039	.252	**.788**	-.027	**.862**	-.440	**-.738**	.574	**-.584**			
Al	-.106	-.136	-.483	-.465	-.337	-.469	.060	.178	-.360	.223	-.423		
Y	-.221	.241	**-.631**	-.402	**-.719**	-.464	-.395	.534	.193	.130	-.159	.088	
Ce	.266	.478	.095	.161	-.445	.355	-.072	-.299	.800	-.771	.497	-.372	.323

FIGURE CAPTIONS

Figure 1. The Ratak Chain of the Marshall Islands. Ship trackline indicated by the solid line.

Figure 2. Sample location map (bathymetry modified from Chase and Menard, 1973). Contours are in fathoms.

Figure 3. Location of seismic-reflection profiles discussed in the text. These profiles are labeled A, B, etc.

Figure 4. 80-in^3 seismic-reflection profile A collected on the west flank of Majuro Atoll (see Figure 3 for location) and interpretive sketch.

Figure 5. 80-in^3 seismic-reflection profile B collected over Erikub Seamount and interpretive sketch (See Figure 3 for location).

Figure 6. 80-in^3 seismic-reflection profile C collected over the northern flank of Jemo Island (Location shown on Figure 3) and interpretive sketch.

Figure 7. 138-in^3 seismic-reflection profile D collected over Utirik Seamount (See Figure 3 for location) and interpretive sketch.

Figure 8. 148-in^3 seismic-reflection profile E collected over Bikar Guyot and interpretive sketch (See Figure 3 for location).

Figure 9. 3.5-kHz seismic-reflection profile F collected over Ratak Guyot (See Figure 3 for location). The insert, an 80-in^3 airgun seismic-reflection profile, was collected simultaneously.

Figure 10. A bottom photograph of rippled sand collected during box coring operation BC3, station 17. The trigger weights for the box corer located near the top of the photograph are 30-cm long.

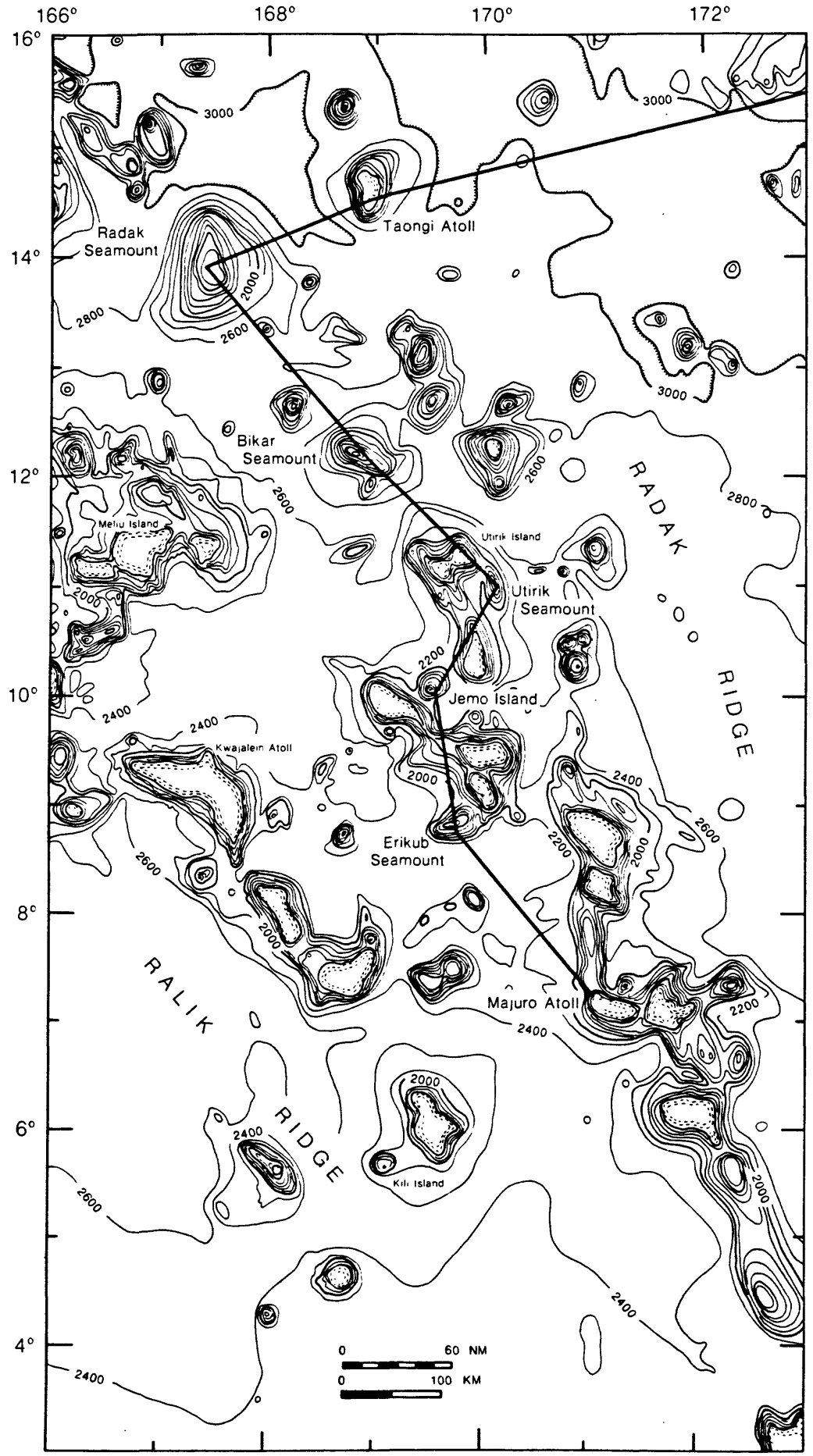
166°
168°
170°
172°
16°
14°
12°
10°
8°
6°
4°
Radak Seamount
Taongi Atoll
Bikar Seamount
Meliu Island
Utirik Island
Utirik Seamount
Jemo Island
Kwajalein Atoll
Erikub Seamount
Majuro Atoll
Kili Island
RADAK RIDGE
RALIK RIDGE
3000
2800
2600
2400
2200
2000
0 60 NM
0 100 KM

Figure 1.

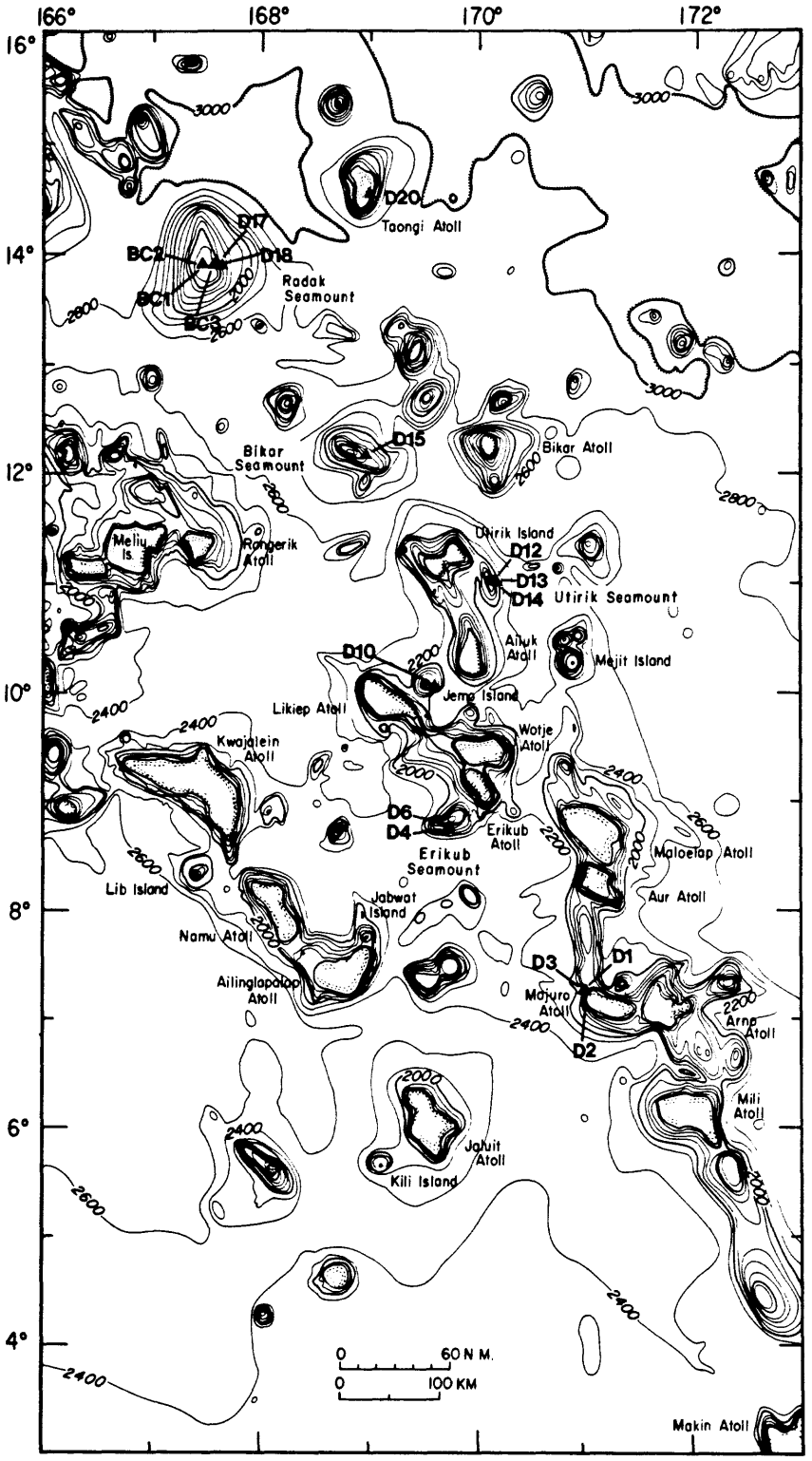
166°
168°
170°
172°
16°
14°
12°
10°
8°
6°
4°
3000
2800
2600
2400
2200
2000
D20
Taongi Atoll
D17
BC2
D18
Radak Seamount
BC1
BC3
D15
Bikar Seamount
Bikar Atoll
Meliu Is.
Rongerik Atoll
Utirik Island
D12
D13
D14
Utirik Seamount
D10
Ailuk Atoll
Mejit Island
Jemo Island
Likiep Atoll
Wotje Atoll
Kwajalein Atoll
D6
D4
Erikub Atoll
Erikub Seamount
Maloelap Atoll
Aur Atoll
Lib Island
Jabwat Island
Namu Atoll
Ailinglapalap Atoll
D3
D1
Majuro Atoll
D2
Arno Atoll
Mili Atoll
Jaluit Atoll
Kili Island
0 60 N M.
0 100 KM
Makin Atoll

Figure 2.

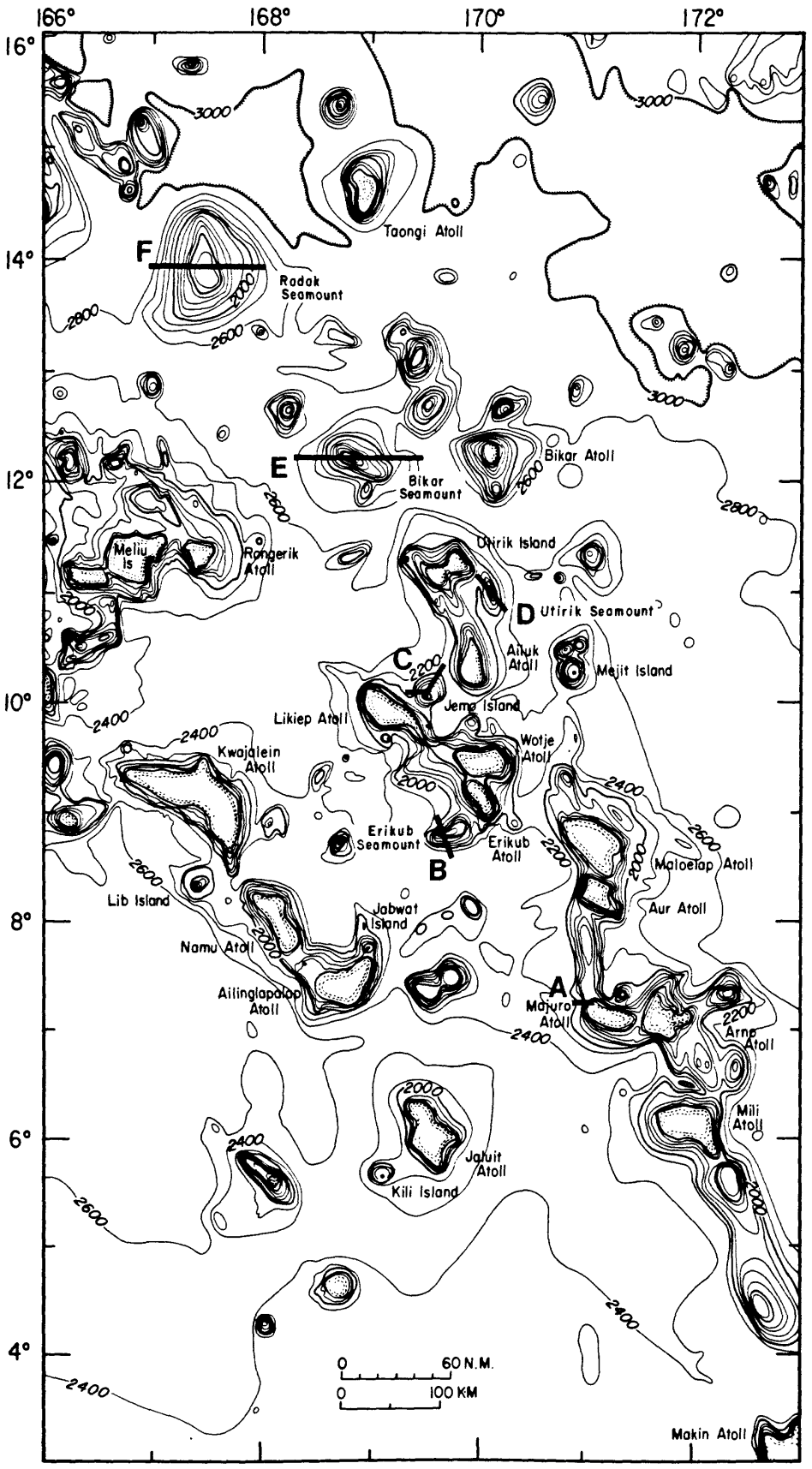
166°
168°
170°
172°
16°
14°
12°
10°
8°
6°
4°
Taongi Atoll
Radak Seamount
F
E
Bikar Seamount
Bikar Atoll
Utirik Island
D
Utirik Seamount
Meliu Is
Rongerik Atoll
C
Ailuk Atoll
Mejit Island
Jemo Island
Likiep Atoll
Wotje Atoll
Kwajalein Atoll
Erikub Seamount
Erikub Atoll
B
Maloelap Atoll
Aur Atoll
Lib Island
Jabwat Island
Namu Atoll
Ailinglapalap Atoll
A
Majuro Atoll
Arno Atoll
Mili Atoll
Jaluit Atoll
Kili Island
0 60 N.M.
0 100 KM
Makin Atoll
3000
2800
2600
2400
2200
2000

Figure 3.

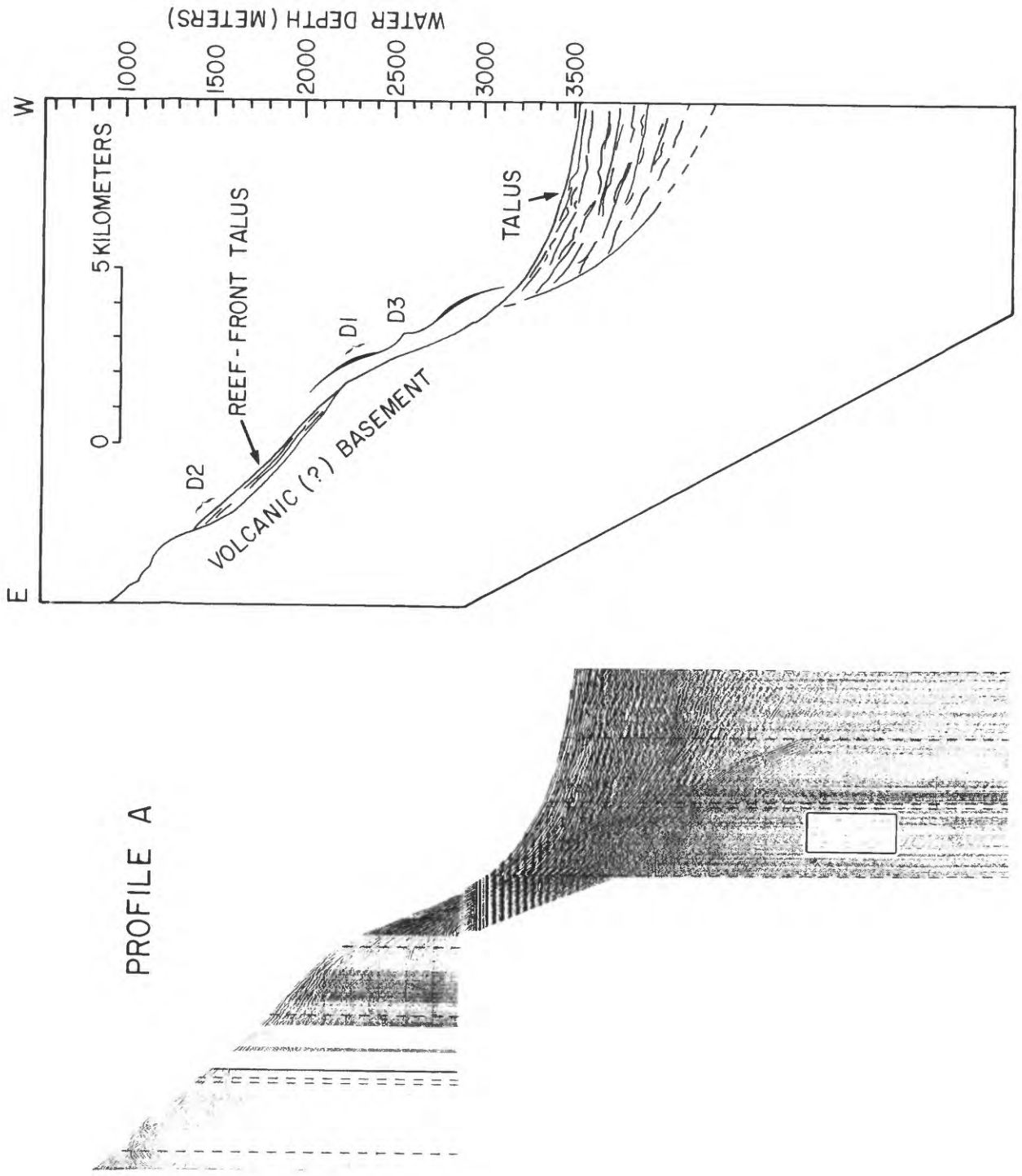
WATER DEPTH (METERS)
1000
1500
2000
2500
3000
3500
W
E
5 KILOMETERS
0
REEF-FRONT TALUS
TALUS
D1
D2
D3
VOLCANIC (?) BASEMENT
PROFILE A

Figure 4.

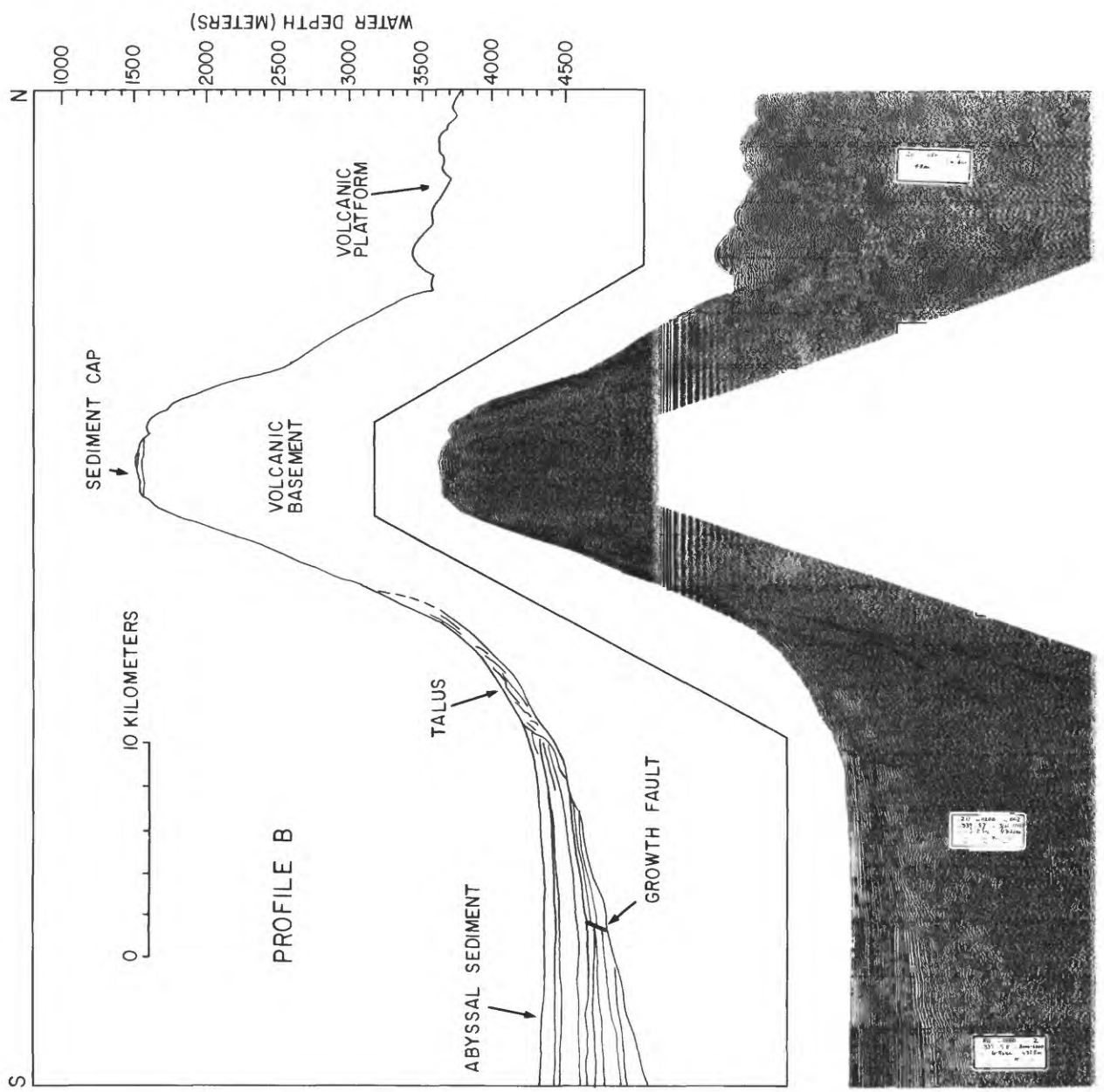
WATER DEPTH (METERS)
1000
1500
2000
2500
3000
3500
4000
4500
N
S
SEDIMENT CAP
VOLCANIC PLATFORM
VOLCANIC BASEMENT
TALUS
ABYSSAL SEDIMENT
GROWTH FAULT
PROFILE B
0
10 KILOMETERS

Figure 5.

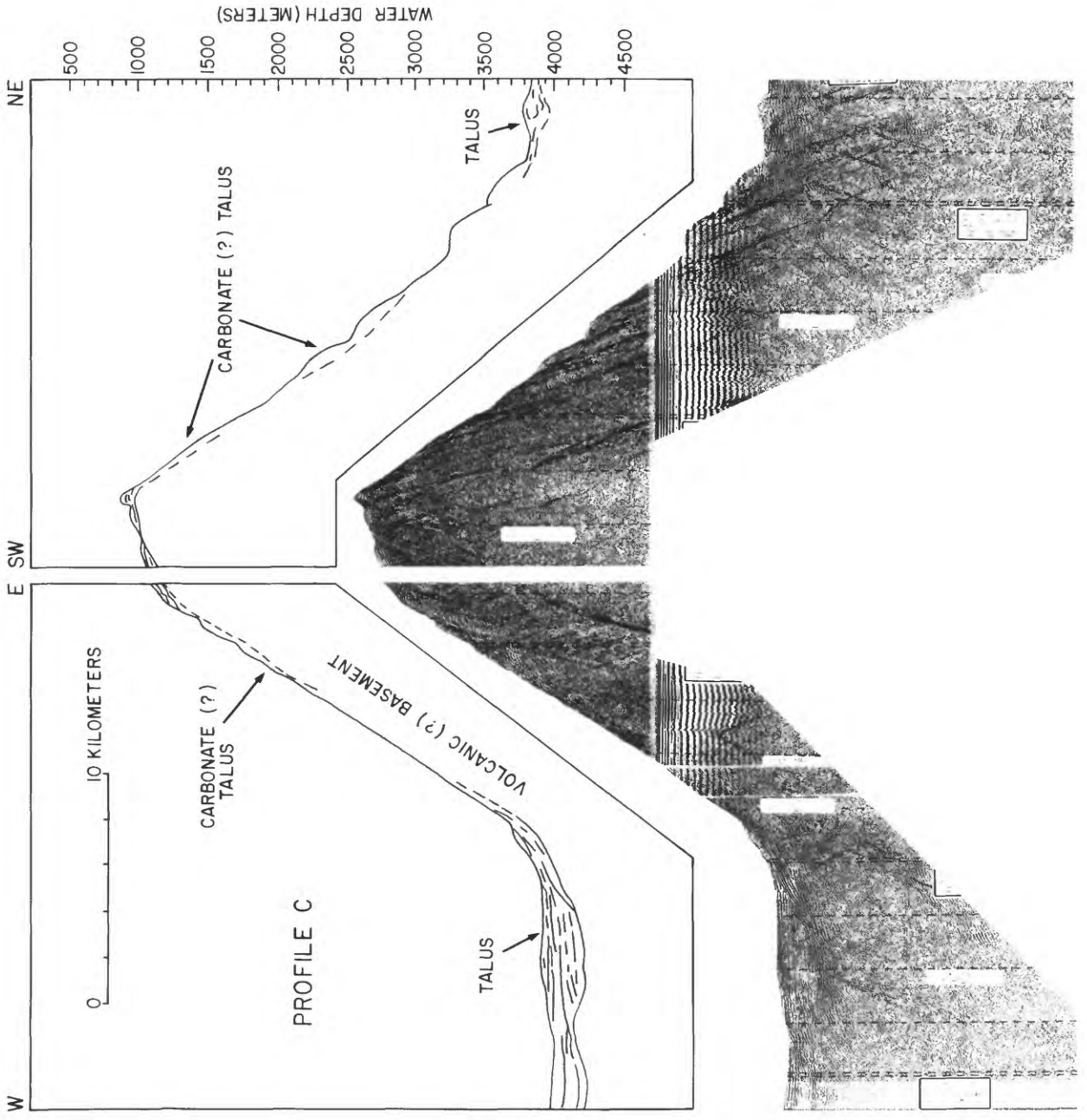
WATER DEPTH (METERS)
500
1000
1500
2000
2500
3000
3500
4000
4500
NE
SW
E
W
TALUS
CARBONATE (?) TALUS
VOLCANIC (?) BASEMENT
CARBONATE (?) TALUS
TALUS
10 KILOMETERS
0
PROFILE C

Figure 6.

SE
NW
WATER DEPTH (METERS)
1000
1500
2000
2500
0
10 KILOMETERS
SEDIMENT CAP
FLANK OF UTIRIK IS.
VOLCANIC(?) PINNACLES
VOLCANIC(?) BASEMENT
UTIRIK SEAMOUNT
PROFILE D

Figure 7.

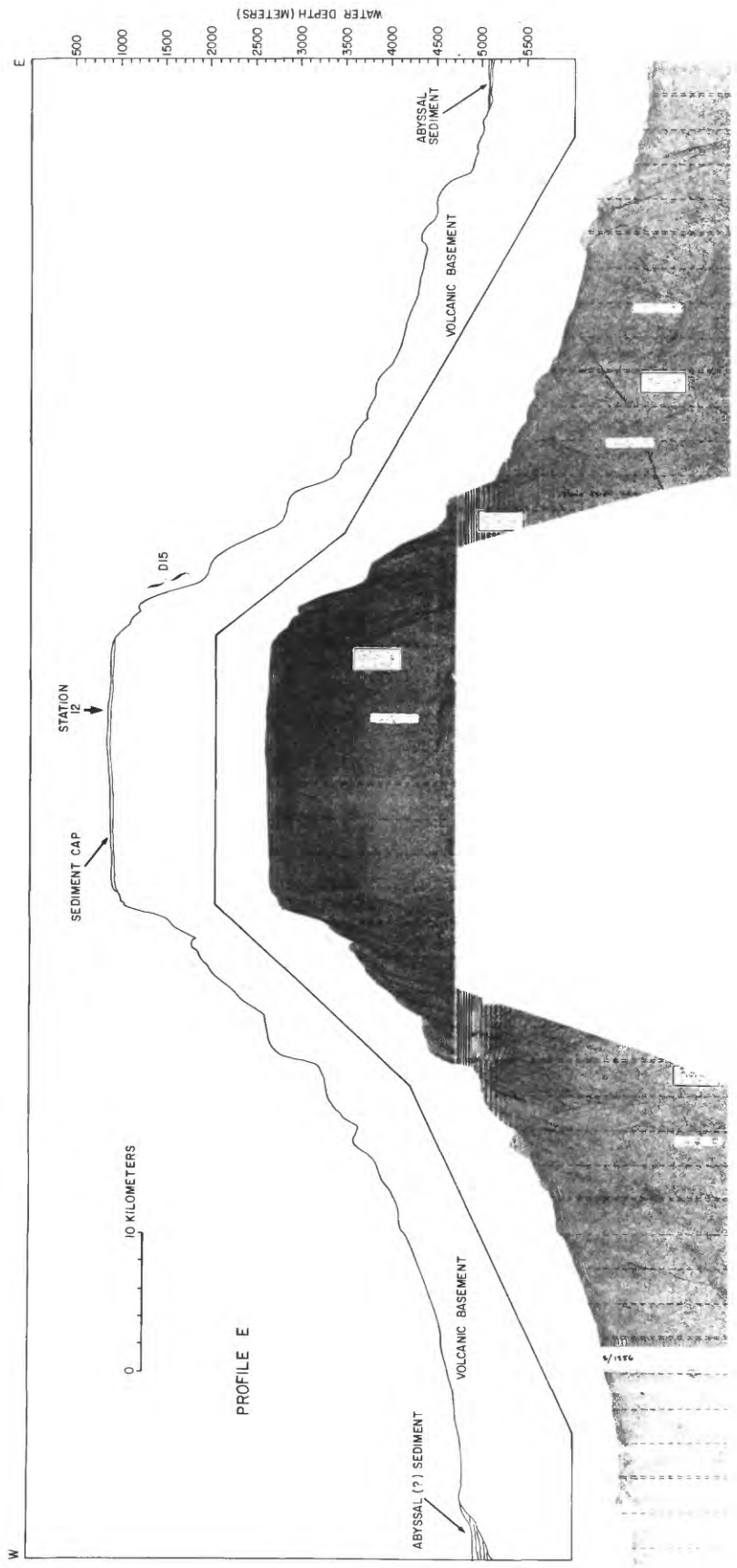
WATER DEPTH (METERS)
500
1000
1500
2000
2500
3000
3500
4000
4500
5000
5500
E
W
ABYSSAL SEDIMENT
VOLCANIC BASEMENT
D15
STATION 12
SEDIMENT CAP
0
10 KILOMETERS
PROFILE E
VOLCANIC BASEMENT
ABYSSAL (?) SEDIMENT

Figure 8.

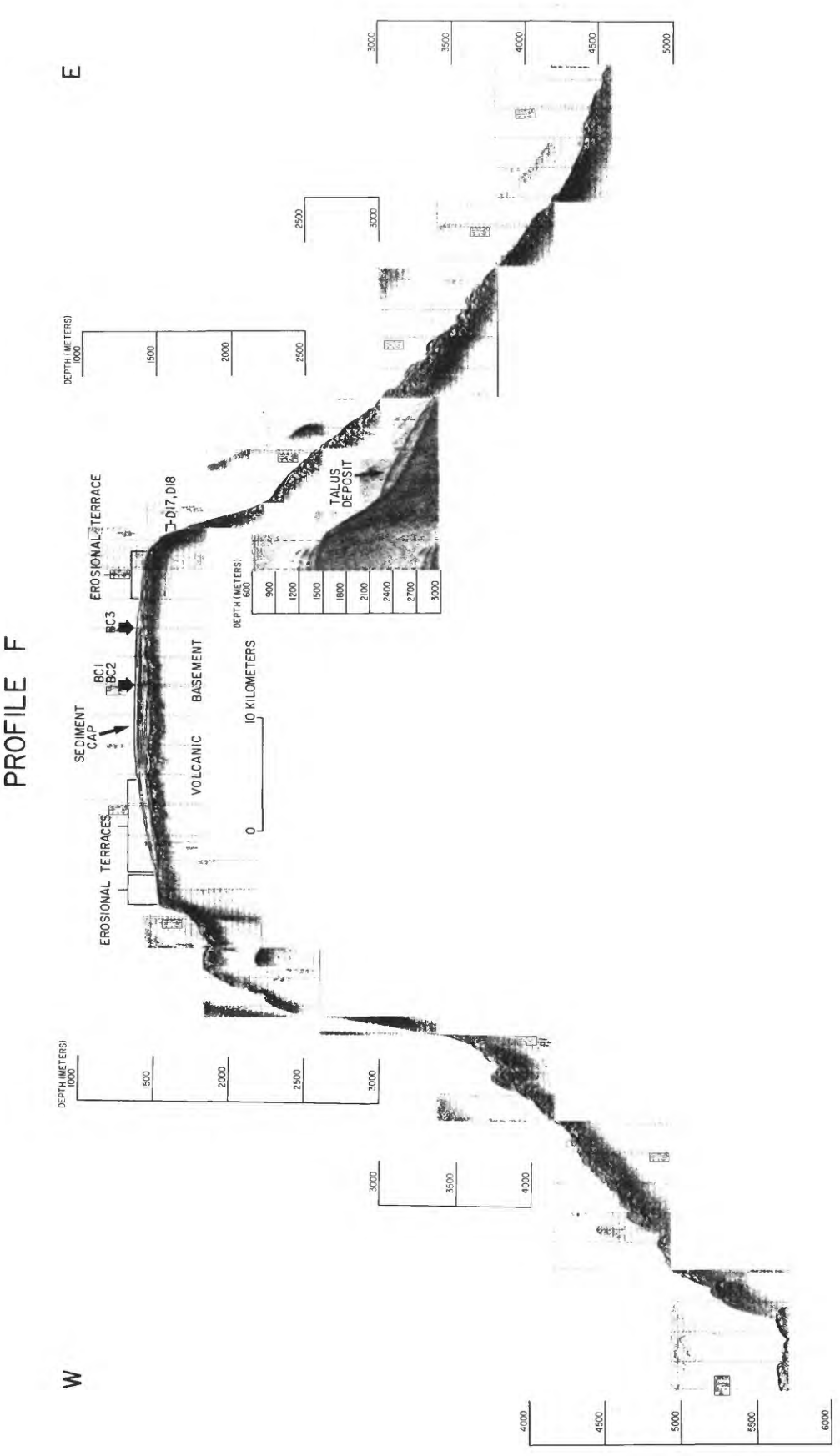
PROFILE F
W
E
DEPTH (METERS)
1000
1500
2000
2500
3000
3500
4000
4500
5000
5500
6000
EROSIONAL TERRACES
SEDIMENT CAP
BC1
BC2
BC3
VOLCANIC BASEMENT
EROSIONAL TERRACE
D17, D18
TALUS DEPOSIT
0
10 KILOMETERS
DEPTH (METERS)
600
900
1200
1500
1800
2100
2400
2700
3000

Figure 9.

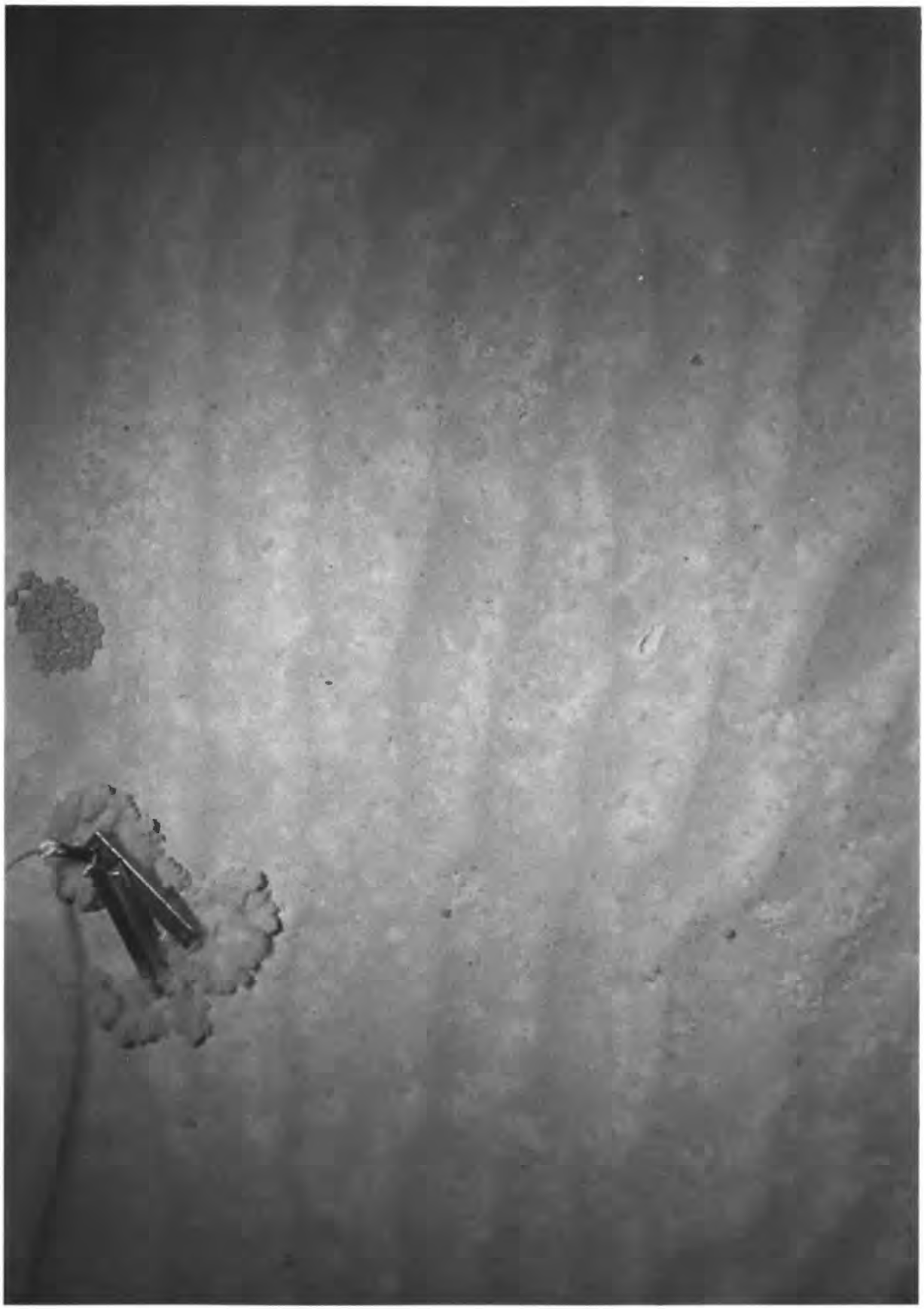

Figure 10.